

## CONSTRAINTS ON THE LEPTON ASYMMETRY AND RADIATION ENERGY DENSITY: IMPLICATIONS FOR PLANCK

L. A. POPA, P. STEFANESCU, A. VASILE

*ISS Institute for Space Sciences Bucharest-Magurele, Ro-077125 Romania, e-mail:  
lpopa@venus.nipne.ro, pstep@venus.nipne.ro, avasile@venus.nipne.ro*

(Received June 5, 2008)

*Abstract.* By using most of the present Cosmic Microwave Background (CMB) and Large Scale Structure (LSS) measurements and the Big Bang Nucleosynthesis (BBN) constraints on the primordial helium abundance,  $Y_p$ , we set bounds on the radiation content of the Universe and neutrino properties. We consider lepton asymmetric cosmological models and we find that present CMB and LSS data constraint the neutrino degeneracy parameter at  $\xi_\nu$  (and consequently the lepton asymmetry of the neutrino background  $L_\nu$ ),  $\Delta N_{oth}^{eff}$  the variation of the relativistic degrees of freedom due to possible other physical processes that occurred between BBN and structure formation epoch, the contribution to the effective number of relativistic neutrino species  $\Delta N_{eff}$  and  $Y_p$  (2- $\sigma$  errors), better than older datasets or CMB data alone and the standard value of  $Y_p$ , 0.24, relaxing the stringent BBN constraint on the neutrino degeneracy parameter.

We forecast that the CMB temperature and polarization maps observed with high angular resolutions and sensitivity by the future Planck Mission will constraint  $Y_p$  in agreement with its most stringent limits given by the BBN and also the neutrino degeneracy parameter, not excluding the possibility of larger lepton asymmetry. This work has been done on behalf of Planck-LFI activities.

*Key words:* CMBR theory, dark matter, cosmological neutrinos, gravitational lensing.

### 1. INTRODUCTION

The radiation budget of the Universe relies on a strong theoretical prejudice: apart from the Cosmic Microwave Background (CMB) photons, the relativistic background would consist of neutrinos and of possible contributions from other relativistic relicts. The main constraints on the radiation energy density come either from the very early Universe, where the radiation was the dominant source of energy, or from the observation of cosmological perturbations which carry the information about the time equality between matter and radiation.

In particular, the primordial light element abundance predictions in the standard theory of the Big Bang Nucleosynthesis (BBN) [1, 2, 3, 4] depend on the baryon-to photon ratio,  $\eta_B$ , and the radiation energy density at the BBN epoch

(energy density of order  $\text{MeV}^4$ ), usually parametrized by the effective number of relativistic neutrino species,  $N^{\text{eff}}$ .

Meanwhile, the number of active neutrino flavors have been fixed by  $Z^0$  boson decay width to  $N_\nu = 2.944 \pm 0.012$  [4] and the combined study of the incomplete neutrino decoupling and the QED corrections indicate that the number of relativistic neutrino species is  $N_\nu^{\text{eff}} = 3.046$  [5]. Any departure of  $N_{\text{eff}}$  from this last value would be due to non-standard neutrino features or to the contribution of other relativistic relics. The solar and atmospheric neutrino oscillation experiments [6, 7] indicate the existence of non-zero neutrino masses in eV range.

There are also indications of neutrino oscillations with larger mass-squared difference, coming from the short base-line oscillation experiments [8, 9], that can be explained by adding one or two sterile neutrinos with eV-scale mass to the standard scheme with three active neutrino flavors (see Ref.[10] for a recent analysis). Such results have impact on cosmology because sterile neutrinos can contribute to the number of relativistic degrees of freedom at the Big Bang Nucleosynthesis [11]. These models are subject to strong bounds on the sum of active neutrino masses from the combination of various cosmological data sets [12, 13], ruling out a thermalized sterile neutrino component with eV mass [14, 15].

However, there is the possibility to accommodate the cosmological observations with data from short base-line neutrino oscillation experiments by postulating the existence of a sterile neutrino with the mass of few keV having a phase-space distribution significantly suppressed relative to the thermal distribution. For both, non-resonant zero lepton number production and enhanced resonant production with initial cosmological lepton number, keV sterile neutrinos are produced via small mixing angle oscillation conversion of thermal active neutrinos [16]. Sterile neutrino with mass of few keV provides also a valuable Dark Matter (DM) candidate [17, 18, 19, 20], alleviating the accumulating contradiction between the  $\Lambda\text{CDM}$  model predictions on small scales and observations, by smearing out the small scale structure.

On the other hand, the possible existence of new particles such as axions and gravitons, the time variation of the physical constants and other non-standard scenarios (see e.g.[21] and references therein) could contribute to the radiation energy density at BBN epoch.

At the same time, more phenomenological extensions to the standard neutrino sector have been studied, the most natural being consideration of the leptonic asymmetry [22, 23, 24], parametrized by the neutrino degeneracy parameter  $\xi_\nu = \mu_\nu / T_{\nu_0}$  [ $\mu_\nu$  is the neutrino chemical potential and  $T_{\nu_0}$  is the present temperature of the neutrino background,  $T_{\nu_0} / T_{\text{CMB}} = (4/11)^{1/3}$ ].

Although the standard model predicts the leptonic asymmetry of the same order as the baryonic asymmetry,  $B \sim 10^{-10}$ , there are many particle physics scenario in which a leptonic asymmetry much larger can be generated [25, 26]. One of the cosmological implications of a larger leptonic asymmetry is the possibility to

generate small baryonic asymmetry of the Universe through the non-perturbative (sphaleron) processes [27, 28, 29]. Therefore, distinguishing between a vanishing and non-vanishing  $\xi_\nu$  at the BBN epoch is a crucial test of the standard assumption that sphaleron effects equilibrate the cosmic lepton and baryon asymmetries.

The measured neutrino mixing parameters implies that neutrinos reach the chemical equilibrium before BBN [30, 31, 32] so that all neutrino flavors are characterized by the same degeneracy parameter,  $\xi_\nu$ , at this epoch.

The most important impact of the leptonic asymmetry on BBN is the shift of the beta equilibrium between protons and neutrons and the increase of the radiation energy density parametrized by:

$$\Delta N^{eff}(\xi_\nu) = 3 \left[ \frac{30}{7} \left( \frac{\xi_\nu}{\pi} \right)^2 + \frac{15}{7} \left( \frac{\xi_\nu}{\pi} \right)^4 \right]. \quad (1)$$

The BBN constraints on  $N^{eff}$  have been recently reanalyzed by comparing the theoretical predictions and experimental data on the primordial abundances of light elements, using the baryon abundance derived from the WMAP 3-year (WMAP3) CMB temperature and polarization measurements [33, 34, 35]:  $\eta_B = 6.14 \times 10^{-10} (1.00 \pm 0.04)$ . In particular, the  ${}^4\text{He}$  abundance,  $Y_p$ , is quite sensitive to the value of  $N^{eff}$ . The analysis of Ref. [36], the conservative error analysis of helium abundance,  $Y_p = 0.249 \pm 0.009$  [37], yielded to  $N^{eff} = 3.1_{-1.2}^{+1.4}$  ( $2\text{-}\sigma$ ) in good agreement with the standard value, but still leaving some room for non-standard values, while more stringent error bars of helium abundance,  $Y_p = 0.2516 \pm 0.0011$  [38], led to  $N^{eff} = 3.32_{-0.24}^{+0.23}$  ( $2\text{-}\sigma$ ) [39].

The stronger constraints on the degeneracy parameter obtained from BBN [40] gives  $-0.04 < \xi < 0.07$  ( $1\text{-}\sigma$ ), adopting the conservative error analysis of  $Y_p$  of Ref. [37] and  $\xi = 0.024 \pm 0.0092$  ( $1\text{-}\sigma$ ), adopting the more stringent error bars of  $Y_p$  of Ref. [41].

The CMB anisotropies and LSS matter density fluctuations power spectra carry the signature of the energy density of the Universe at the time of matter-radiation equality (energy density of order  $\text{eV}^4$ ), making possible the measurement of  $N^{eff}$  through its effects on the growth of cosmological perturbations.

More effective number of relativistic neutrino species enhances the integrated Sachs-Wolfe effect on the CMB power spectrum, leading to a higher first acoustic Doppler peak amplitude. Also, the delay of the epoch of matter-radiation equality shifts the LSS matter power spectrum turnover position toward larger angular scales, suppressing the power at small scales. In particular, for the leptonic asymmetric models, the neutrino mass is lighter than in the symmetric case. This leads to changes in neutrino free-streaming length and neutrino Jeans mass due to the increase of the neutrino velocity dispersion [42, 43].

After WMAP3 data release, there are many works aiming to constrain  $N_{\text{eff}}$  from cosmological observations [14, 33, 36, 44, 45, 46]. Their results suggest large values for  $N_{\text{eff}}$  within  $2\text{-}\sigma$  interval, some of them not including the standard value  $N_{\text{eff}}^{\text{std}} = 3.046$  [14, 33, 36]. Recently Ref. [47] argues that the discrepancies are due to the treatment of the scale-dependent biasing in the galaxy power spectrum inferred from the main galaxy sample of the Sloan Digital Sky Survey data release 2 (SDSS-DR2) [48, 49] and the large fluctuation amplitude reconstructed from the Lyman- $\alpha$  forest data [50] relative to that inferred from WMAP3.

Discrepancies between BBN and cosmological data results on  $N_{\text{eff}}$  was interpreted as  $2\text{-}\sigma$  evidence of the fact that further relativistic species are produced by particles decay between BBN and structure formation [45, 46]. Other theoretical scenarios include the violation of the spin-statistics in the neutrino sector [51], the possibility of an extra interaction between the dark energy and radiation or dark matter, the existence of a Brans-Dicke field which could mimic the effect of adding extra relativistic energy density between BBN and structure formation epochs [52].

The extra energy density can be split in two distinct uncorrelated contributions, first due to net lepton asymmetry of the neutrino background and second due to the extra contributions from other unknown processes:

$$\Delta N_{\text{eff}} = \Delta N_{\text{eff}}(\xi) + \Delta N_{\text{oth}}^{\text{eff}}. \quad (2)$$

The aim of this paper is to obtain bounds on the neutrino lepton asymmetry and on the extra radiation energy density by using most of the existing CMB and LSS measurements and self-consistent BBN priors on  $Y_p$ . We also compute the sensitivity of the future Planck experiment [53] for these parameters testing the restrictions on cosmological models with extra relativistic degrees of freedom expected from high precision CMB temperature and polarization anisotropy measurements.

The paper is organized as follows: Section 2 contains a review on the lepton asymmetric cosmological models and the BBN theory, Section 3 is devoted to a summary data analysis method while in Section 4 we discuss our results. We draw our main conclusions in Section 5.

## 2. LEPTONIC ASYMMETRIC COSMOLOGICAL MODELS AND THE BBN THEORY

The density perturbations in leptonic asymmetric cosmological models have been discussed in literature [42, 43, 54, 55]. We applied them to modify the Boltzmann Code for Anisotropies in the Microwave Background (CAMB) [56, 57, 58] to compute the CMB temperature and polarization anisotropies power spectra and LSS matter density fluctuations power spectra for the case of three degenerate neutrinos/antineutrinos with mass  $m_\nu$  and degeneracy parameter  $\xi_\nu$ . As neutrinos

reach their approximate chemical potential equilibrium before BBN epoch [30, 31, 32], we consider in our computation that all three flavors of neutrinos/antineutrinos have the same degeneracy parameter  $\xi_\nu$ . For simplicity, we also consider all three neutrino/antineutrino flavors with the same mass  $m_\nu$ .

When the Universe was hot enough, neutrinos and antineutrinos of each flavor behave like relativistic particles with Fermi-Dirac phase space distributions:

$$f_\nu(q) = \frac{1}{e^{E_\nu/T_\nu - \xi_\nu} + 1}, \quad f_{\bar{\nu}}(q) = \frac{1}{e^{E_\nu/T_\nu - \xi_\nu} + 1}, \quad (3)$$

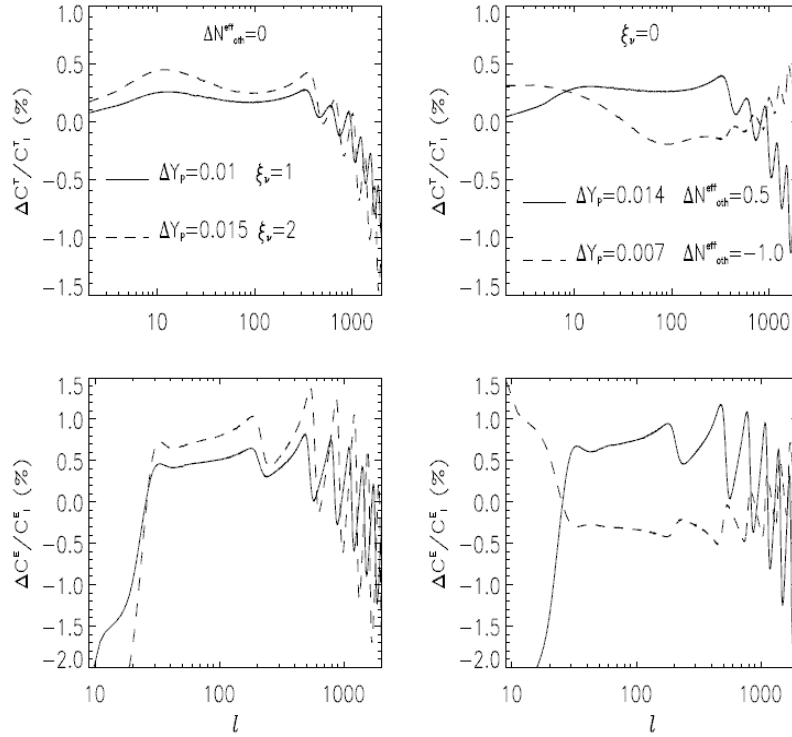


Fig. 1. - The CMB temperature (top panels) and polarization (bottom panels) percentage differences corresponding to different helium fractions variations  $\Delta Y_p$  with respect to the standard value

$Y_p = 0.248$  for:  $\xi_\nu \neq 0$  and  $\Delta N_{oth}^{eff} = 0$  (left panels) and  $\Delta N_{oth}^{eff} \neq 0$  and  $\xi_\nu = 0$  (right panels).

All other parameters are fixed to the values of our fiducial model.

where  $E_\nu = \sqrt{q^2 + a^2 m_\nu^2}$  is one flavor neutrino/antineutrino energy and  $q = ap$  is the comoving momentum. Hereafter,  $a$  is the cosmological scale factor ( $a_0 = 1$  today). The mean energy density and pressure of one flavor of massive degenerated neutrinos and antineutrinos can be written as:

$$\rho_{\nu} + \rho_{\bar{\nu}} = (k_B T_{\nu})^4 \int_0^{\infty} \frac{d^3 q}{(2\pi)^3} q^2 E_{\nu} (f_{\nu}(q) + f_{\bar{\nu}}(q)), \quad (4)$$

$$3(P_{\nu} + P_{\bar{\nu}}) = (k_B T_{\nu})^4 \int_0^{\infty} \frac{d^3 q}{(2\pi)^3} \frac{q^2}{E_{\nu}} (f_{\nu}(q) + f_{\bar{\nu}}(q)). \quad (5)$$

We modify in CAMB the expressions for the energy density and the pressure in the relativistic and non-relativistic limits for the degenerate case [43] and follow the standard procedure to compute the perturbed quantities by expanding the phase space distribution function of neutrinos and antineutrinos into homogeneous and perturbed inhomogeneous components [58, 59, 60]. Since the gravitational source term in the Boltzmann equation is proportional to the logarithmic derivative of the neutrino distribution function with respect to comoving momentum,  $d \ln(f_{\nu} + f_{\bar{\nu}}) / d \ln q$ , we also modify this term to account for  $\xi_{\nu} \neq 0$  [43, 54].

As mentioned in the first section, the BBN theory gives strong constraints on  $N^{eff}$  at this epoch by comparing the measured light element abundance with the theoretical predictions. The only free parameter is the baryon to photon ratio,  $\eta_B = n_b/n_{\gamma}$ , that is obtained from the CMB observation of  $\Omega_b h^2$ .

In particular, the  ${}^4\text{He}$  mass fraction,  $Y_p$ , affects the CMB angular power spectra through its impact on different evolution phases of the ionization/recombination history [61].

We modify the recombination routine recfast [62] of the CAMB code to explicitly account for the dependence of  $Y_p$  on  $\Omega_b h^2$  and on  $\Delta N_{eff}$  as defined in equation (2), as previously suggested in Ref. [63], by adopting the fitting formula [64]:

$$10Y_p = \left( \sum_{n=1}^8 a_n x^{n-1} + \sum_{n=1}^8 b_n x^{n-1} \Delta N^{eff} + \sum_{n=1}^8 c_n x^{n-1} (\Delta N^{eff})^2 + \sum_{n=1}^8 d_n x^{n-1} (\Delta N^{eff})^3 \right) \times \exp \left( \sum_{n=1}^6 e_n x^n \right), \quad (6)$$

where  $x = \log_{10}(10^{10}\eta)$  and  $10^{10} \eta = 273.49 \Omega_b h^2$ . The coefficients  $a_n$ ,  $b_n$ ,  $c_n$ ,  $d_n$  and  $e_n$  are given in Ref. [64]. The standard prediction of BBN  $Y_p = 0.248$  is obtained for  $\Delta N^{eff} = 0$ . According to Ref. [64], the accuracy of this fitting formula is better than 0.05% for the range  $5.48 \times 10^{-10} < \eta_B < 7.12 \times 10^{-10}$  ( $0.02 < \Omega_b h^2 < 0.026$ ) which corresponds to the 3- $\sigma$  interval obtained by WMAP3 and  $-3 < \Delta N^{eff} < 3$ .

Figure 1 presents the CMB temperature and polarization percentage differences corresponding to the different variations of the helium fraction,  $\Delta Y_p$ , with respect to the standard value  $Y_p = 0.248$  obtained for  $\xi \neq 0$  and  $\Delta N_{oth}^{eff} = 0$  and

$\Delta N_{oth}^{eff} \neq 0$  and  $\xi = 0$ . The impact of the percent change in  $Y_p$  on the ionization/recombination history has a net impact on the CMB temperature and polarization power spectra at percent level.

### 3. ANALYSIS

We use the CosmoMC Monte Carlo Markov Chain (MCMC) public package [65] modified for our extended 6+3 parameter space to sample from the posterior distribution giving the following experimental datasets.

The Cosmic Microwave Background (CMB): We use the WMAP3 data [33, 34, 35] complemented with the CMB data from Boomerang [66, 67], ACBAR [68] and CBI [69] experiments.

Large Scale Structure (LSS): The power spectrum of the matter density fluctuations has been inferred from the galaxy clustering data of the Sloan digital Sky Survey (SDSS) [48, 49, 70, 71] and Two-degree Field Galaxy Redshift Survey (2dFGRS) [72].

In particular, the luminous red galaxies (LRG) sample from the SDSS data release 5 (SDSS-DR5) has more statistical significance [70, 71] than the spectrum retrieved from the SDSS main galaxy sample from data release 2 (SDSS-DR2) [48, 49] eliminating the existing tension between the power spectra from SDSS-DR2 and 2dFGRS. For this reason we consider in our analysis the matter power spectra from SDSS-LRG and 2dFGRS. We consider SDSS-LRG data up to  $k_{max} \sim 0.2h \text{ Mpc}^{-1}$  and the 2dFGRS data up to  $k_{max} \sim 0.14h \text{ Mpc}^{-1}$ . We apply the corrections due to the non-linearity behavior and scale dependent bias as indicated in Ref.[70], connecting the linear matter power spectrum,  $P_{lin}(k)$ , and the galaxy power spectrum,  $P_{gal}(k)$ , by:

$$P_{gal}(k) = b^2 \frac{1 + Q_{nl} k^2}{1 + 1.4k} P_{lin}(k), \quad (7)$$

where the free parameters  $b$  and  $Q_{nl}$  are marginalized.

Type Ia Supernovae (SNIa): We also use the luminosity distance measurements of distant Type Ia supernovae obtained by Supernova Legacy Survey (SNLS) [73] and the Hubble Space Telescope [74].

Hubble Space Telescope key project (HST): We impose priors on the Hubble constant  $H_0 = 72 \pm 8 \text{ km s}^{-1} \text{ Mpc}^{-1}$  from HST key project [75].

BBN constraints on  $Y_p$ : We use the BBN constraints on  $Y_p$  as given in equation (7), allowing  $\Omega_b h^2$  and  $\Delta N^{eff}$  to span the following ranges:  $0.02 < \Omega_b h^2 < 0.026$  and  $-3 < \Delta N^{eff} < 3$ .

Hereafter, we will denote WMAP3+SDSS-DR5+2dFGRS+SNIa+HST+BBN data set as WMAP3+All.

We perform our analysis in the framework of the extended  $\Lambda$ CDM cosmological model described by 6 + 3 free parameters:

$$\Theta = \left( \underbrace{\Omega_b h^2, \Omega_{cdm} h^2, \theta_s, \tau, n_s, A_s}_{\text{standard}}, f_\nu, \xi_\nu, \Delta N_{oth}^{eff} \right). \quad (8)$$

Here  $\Omega_b h^2$  and  $\Omega_{cdm} h^2$  are the baryonic and cold dark matter energy density parameters,  $\theta_s$  is the ratio of the sound horizon distance to the angular diameter distance,  $\tau$  is the reionization optical depth,  $n_s$  is the scalar spectral index of the primordial density perturbation power spectrum and  $A_s$  is its amplitude at the pivot scale  $k^* = 0.05 \text{ hMpc}^{-1}$ .

The additional three parameters denote the neutrino energy density fraction  $f_\nu$ , the neutrino degeneracy parameter  $\xi_\nu$  and the extra contributions from other unknown processes  $\Delta N_{oth}^{eff}$ . Table 1 presents the parameters of our model, their fiducial values used to generate the Planck-like simulated power spectra and the prior ranges adopted in the analysis.

For the forecast from Planck-like simulated data we use the CMB temperature ( $T$ ) and polarization ( $P$ ) power spectra of our fiducial cosmological model and the expected experimental characteristics of the Planck frequency channels presented in Table 2 [53].

Table 1

The free parameters of our model, their fiducial values used to generate the Planck-like simulated power spectra and the prior ranges adopted in the analysis

| Parameter              | Fiducial value | Prior range             |
|------------------------|----------------|-------------------------|
| $\Omega_b h^2$         | 0.022          | 0.005 $\rightarrow$ 0.1 |
| $\Omega_{cdm} h^2$     | 0.105          | 0.01 $\rightarrow$ 0.5  |
| $\theta_s$             | 1.04           | 0.5 $\rightarrow$ 5     |
| $\tau$                 | 0.09           | 0.01 $\rightarrow$ 0.3  |
| $n_s$                  | 0.95           | 0.5 $\rightarrow$ 1.3   |
| $\ln[10^{10} A_s]$     | 3              | 2.7 $\rightarrow$ 4     |
| $f_\nu$                | 0.05           | 0 $\rightarrow$ 0.5     |
| $\xi_\nu$              | 0              | 0 $\rightarrow$ 4       |
| $\Delta N_{oth}^{eff}$ | 0.046          | -3 $\rightarrow$ 3      |
| $Y_P$                  | 0.248          |                         |

For each frequency channel we consider an homogeneous detector noise with the power spectrum:

$$N_{l,\nu}^c = (\theta_b \Delta_a)^2 \exp^{l(l+1)\theta_b^2/8\ln 2}, \quad c \in (T, P), \quad (9)$$

where  $\nu$  is the frequency of the channel,  $\theta_b$  is the FWHM of the beam and  $\Delta_c$  are the corresponding sensitivities per pixel. The global noise of the experiment is obtained as:

$$N_l^c = \left[ \sum_{\nu} \left( N_{l,\nu}^c \right)^{-1} \right]^{-1}. \quad (10)$$

In order to interpret the likelihood function,  $\mathcal{L}(\Theta)$ , as probability density we assume uniform prior probability on the parameters  $\Theta$  (i.e. will assume that all values of parameters are equally probable). For each parameter we compute the cumulative distribution function  $C(\Theta) = \int_{\Theta_{\min}}^{\Theta} L(\Theta) d\Theta / \int_{\Theta_{\min}}^{\Theta_{\max}} L d\Theta$  and quote as upper and lower intervals at  $2\text{-}\sigma$  the values at which  $C(\Theta)$  is 0.95 and 0.05 respectively. For the case when  $L(\Theta)$  is zero and  $\Theta$  has a positive values (i.e.  $f_\nu$ , the absolute value of  $\xi_\nu$ ) we quote only the upper limit at  $2\text{-}\sigma$ .

Table 2

The expected experimental characteristics for the Planck frequency channels considered in the paper.  $\Delta_T$  and  $\Delta_p$  are the sensitivities per pixel for temperature and polarization maps

| $\nu$ (GHz) | FWHM(arc minutes) | $\Delta_T$ ( $\mu$ K) | $\Delta_p$ ( $\mu$ K) |
|-------------|-------------------|-----------------------|-----------------------|
| 100         | 9.5               | 6.8                   | 10.9                  |
| 143         | 7.1               | 6.0                   | 11.4                  |
| 217         | 5.0               | 13.1                  | 26.7                  |

## 4. RESULTS

We start by making a consistency check, verifying that by using WMAP3+All data and imposing  $\xi_\nu=0$ ,  $\Delta N_{oth}^{eff} = 0$  and  $Y_p = 0.248$  priors we obtain results in agreement with the ones obtained by WMAP collaboration (Tables 5 and 6 from Ref. [33]).

In order to understand how the extra relativistic energy density and the leptonic asymmetry affect the determination of other cosmological parameters, we compute first the likelihood functions for WMAP3+All by imposing  $\Delta N_{oth}^{eff} = 0$  prior. We then extend our computation over the whole parameter space for WMAP3+All and Planck-like simulated data. In Fig. 2 we compare the marginalized likelihood probabilities obtained for WMAP3+All with  $\Delta N_{oth}^{eff} = 0$  prior with those obtained for WMAP3+All and Planck without priors on  $\Delta N_{oth}^{eff}$ .

The main effect of including the contribution of the extra relativistic energy density is the change in the age of the Universe (and in the Hubble expansion rate) from  $t_0 = 13.81 \pm 0.26$  GYrs to  $t_0 = 13.42^{+1.3}_{-1.42}$  GYrs (2- $\sigma$  errors), effect that is mostly driven by the increased degeneracy between matter and radiation energy densities.

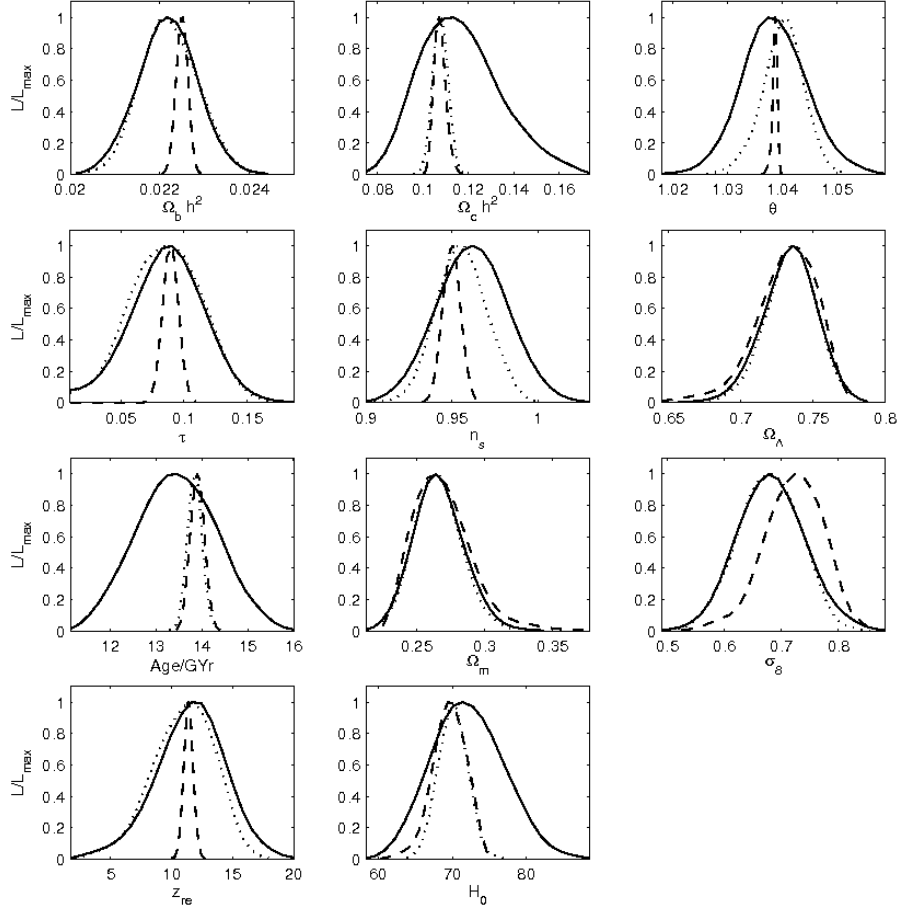


Fig. 2 – The marginalized posterior likelihood probabilities of the main cosmological parameters obtained for: WMAP3+All with  $\Delta N_{oth}^{eff} = 0$  prior (dotted lines) and WMAP3+All (solid lines) and Planck (dashed lines) without priors on  $\Delta N_{oth}^{eff} = 0$ .

We present in Fig. 3 the 2D marginalized 1- $\sigma$  and 2- $\sigma$  allowed regions in  $t_0 - |\xi|$  and  $t_0 - \Delta N_{oth}^{eff}$  planes showing this effect. The 2- $\sigma$  confidence region for the additional number of relativistic relicts is  $-1.207 \leq \Delta N_{oth}^{eff} \leq 2.572$ , for

WMAP3+All, and  $-0.226 \leq \Delta N_{oth}^{eff} \leq 0.236$ , for Planck-like simulated data. The negative values of  $\Delta N_{oth}^{eff}$  are lowering the amplitude of the CMB and LSS power spectra that can be compensated by larger values of the degeneracy parameter.

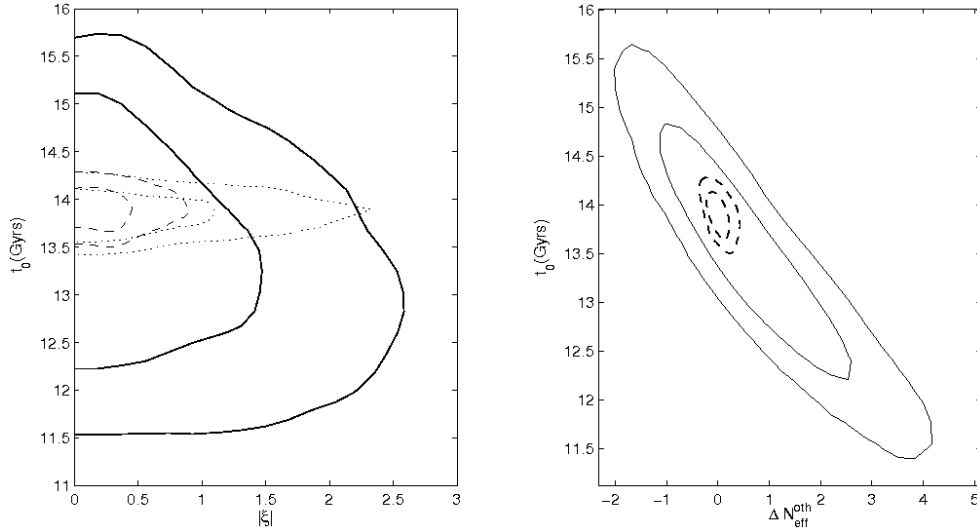


Fig. 3 – The 2D marginalized 1- $\sigma$  and 2- $\sigma$  allowed regions in  $t_0 - |\xi|$  and  $t_0 - \Delta N_{oth}^{eff}$  planes. The dotted curve corresponds to WMAP3+All with  $\Delta N_{oth}^{eff} = 0$  prior. The solid and dashed curves correspond respectively to WMAP3+All and Planck-like simulated data, without priors on  $\Delta N_{oth}^{eff}$ .

We observe during our analysis that the inclusion of an additional number of relativistic relics increases the degeneracy between the cosmological parameters controlling the CMB and LSS power spectra amplitudes.

In Fig. 4 we compare the marginalized likelihood probabilities of the neutrino parameters obtained for WMAP3+All with  $\Delta N_{oth}^{eff}$  prior with those obtained for WMAP3+All and Planck without priors on  $\Delta N_{oth}^{eff}$ . The expectation values and the corresponding errors or the upper limits (2- $\sigma$ ) are presented in Table 3.

We forecast that the precise measurements of the CMB temperature and polarization power spectra from Planck will reduce the degeneracy between  $|\xi|$  and  $\Delta N_{oth}^{eff}$ , allowing better constrains of the scenarios involving additional number of relativistic relics and leptonic asymmetry.

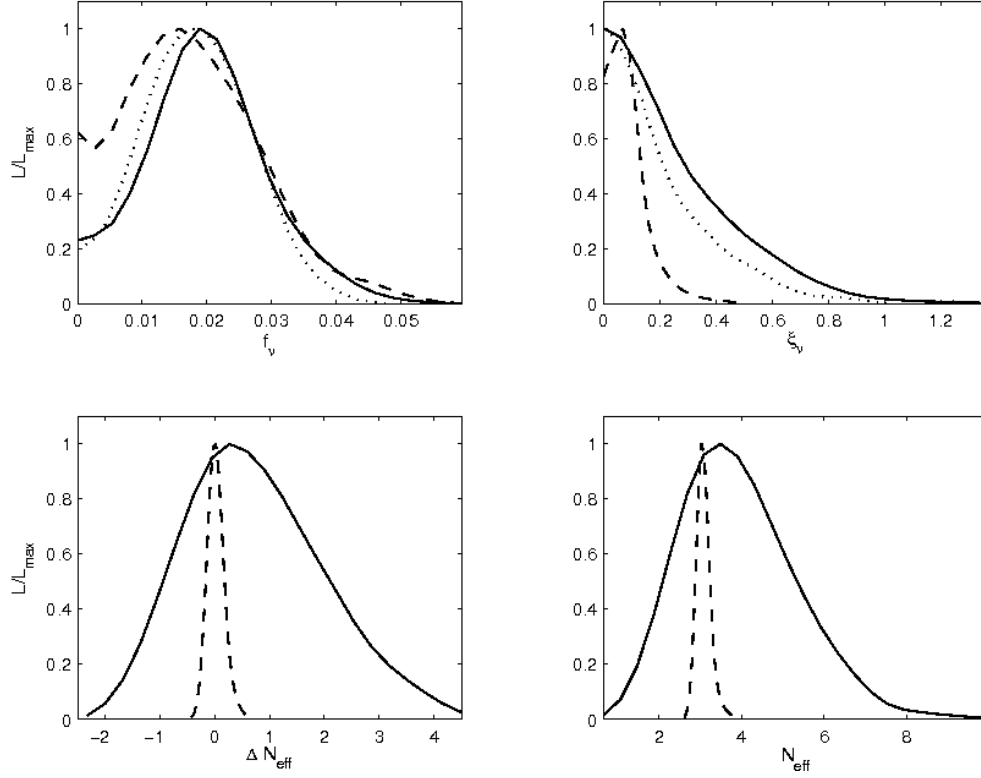


Fig. 4 – The marginalized posterior likelihood probabilities of the neutrino parameters obtained for: WMAP3+All with  $\Delta N_{oth}^{eff}=0$  prior (dotted lines) and WMAP3+All (solid lines) and Planck (dashed lines) without priors on  $\Delta N_{oth}^{eff}$ .

Table 3

Constraints on neutrino parameters and helium mass fraction.  
The errors and the upper limits are at 2- $\sigma$

| Parameter                   | WMAP3+All                  | WMAP3+All                     | PLANCK                        |
|-----------------------------|----------------------------|-------------------------------|-------------------------------|
|                             | $\Delta N_{oth}^{eff} = 0$ | $\Delta N_{oth}^{eff} \neq 0$ | $\Delta N_{oth}^{eff} \neq 0$ |
| $f_\nu$                     | $\leq 0.033$               | $\leq 0.037$                  | $\leq 0.036$                  |
| $ \xi $                     | $\leq 0.590$               | $\leq 0.722$                  | $\leq 0.280$                  |
| $\Delta N_{oth}^{eff}(\xi)$ | $\leq 0.833$               | $\leq 1.243$                  | $\leq 0.158$                  |
| $L_\nu$                     | $\leq 0.474$               | $\leq 0.614$                  | $\leq 0.179$                  |
| $\Delta N_{oth}^{eff}$      | -                          | $0.572^{+1.972}_{-1.780}$     | $0.008^{+0.229}_{-0.234}$     |
| $N_{eff}$                   | $\leq 3.873$               | $3.058^{+1.971}_{-1.178}$     | $2.920^{+0.267}_{-0.216}$     |
| $Y_P$                       | $\leq 0.249$               | $0.249^{+0.014}_{-0.016}$     | $0.247 \pm 0.002$             |

## 5. CONCLUSIONS

In this paper, we set bounds on the radiation content of the Universe and neutrino properties by using most of the present Cosmic Microwave Background (CMB) and Large Scale Structure (LSS) measurements. We also take into account the Big Bang Nucleosynthesis (BBN) constraints on the primordial helium abundance,  $Y_p$ , which prove to be important in the estimation of cosmological parameters from future Planck data, both in non-degenerate and degenerate BBN models; the importance of the self-consistent BBN prior on  $Y_p$  was also emphasized in two other recent analysis [76, 77].

We consider lepton asymmetric cosmological models parametrized by the neutrino degeneracy parameter  $\xi_\nu$  and the variation of the relativistic degrees of freedom,  $\Delta N_{oth}^{eff}$ , due to possible other physical processes that occurred between BBN and structure formation epoch.

We found that present CMB and LSS data together with BBN prior on the primordial helium abundance ( $Y_p$ ) constraints the neutrino degeneracy parameter at  $\xi_\nu \leq 0.722$ , leading to a lepton asymmetric neutrino background of  $L_\nu \leq 0.614$  (2- $\sigma$ ). We also found  $\Delta N_{oth}^{eff} = 0.572_{-1.780}^{+1.972}$ , the contribution to the effective number of relativistic neutrino species  $N^{eff} = 3.058_{-1.178}^{+1.971}$  and a primordial helium abundance  $Y_p = 0.249_{-0.016}^{+0.014}$  (2- $\sigma$  errors). These values represent important improvements over the similar results obtained by using WMAP 1-year together with older LSS data [78] or the WMAP3 data alone [42] and the standard primordial helium abundance value  $Y_p = 0.24$ , relaxing the stringent BBN constraint on the neutrino degeneracy parameter ( $\xi_\nu \leq 0.07$ ).

We observe that, when using WMAP3+All data, an additional number of relativistic relicts brings a substantial degeneracy in the  $\Omega_m - \Omega_r$  plane and a weaker constraint on the age of the Universe; the same degeneracy occurs also between other cosmological parameters under the same conditions. We therefore conclude that the present cosmological data do not favor the variation of the relativistic degrees of freedom,  $\Delta N_{oth}^{eff}$ , due to other possible physical processes that occurred between BBN and matter-radiation equality epoch.

We forecast that the CMB temperature and polarization maps observed with high angular resolutions and sensitivity by the future Planck Mission will constraint the primordial primordial helium abundance at  $Y_p = 0.247 \pm 0.002$  (2- $\sigma$  errors) in agreement with the most stringent limits on  $Y_p$  given by the BBN and the neutrino degeneracy parameter at  $\xi_\nu \leq 0.280$  (2- $\sigma$ ), allowing larger lepton asymmetry models. Also, they will reduce the degeneracy between  $|\xi|$  and  $\Delta N_{oth}^{eff}$  allowing a better distinction between extra radiation energy density coming from an additional number of relativistic relicts and from a lepton asymmetric neutrino background.

*Acknowledgements.* The authors acknowledge the support by the ESA/PECS Contract "Scientific exploitation of Planck-LFI data". We also acknowledge the use of the GRID computing system facility at the Institute for Space Sciences Bucharest and would like to thank the staff working there.

## REFERENCES

1. R. V. Wagoner, W. A. Fowler, F. Hoyle, *Astrophys. J.*, **148**, 3, 1967.
2. K. A. Olive, G. Steigman, T. P. Walker, *Phys. Rep.*, **333**, 389, 2000 [astro-ph/9905320].
3. S. Burles, K. M. Nollett, M. S. Turner, *Astrophys. J.*, **552**, L1, 2001 [astro-ph/0010171].
4. S. Eidelman, et al., *Phys. Lett. B*, **592**, 1, 2004.
5. G. Mangano, G. Miele, S. Pastor, M. Peloso, *Phys. Lett. B*, **534**, 8, 2002 [astro-ph/0111408].
6. Y. Fukuda et al., (Super-Kamiokande Collab.), *Phys. Rev. Lett.*, **81**, 1562, 1998.
7. M. Ambrosio et al., (MACRO Collab.), *Phys. Lett. B*, **434**, 451, 1998 [hep-ex/9807005].
8. C. Athanassopoulos et al., *Phys. Rev. Lett.*, **77**, 3082, 1996 [nucl-ex/9605003].
9. A. A. Aguilar-Arevalo et al., (MiniBooNE Collaboration) 2007 [hep-ex/0704.1500].
10. M. Maltoni, and T. Schwets, 2007 [hep-ex/0705.0107].
11. M. Cirelli, G. Marandella, S. Strumia, F. Vissani, *Nucl. Phys. B*, **708**, 215, 2005 [hep-ph/0403158].
12. S. Hannestad and G. G. Raffelt, *J. Cosmol. Astropart. Phys. JCAP*, **11**, 016, 2006 [astro-ph/0607101].
13. J. Kristiansen, H. K. Eriksen and A. Elgar, *Phys. Rev. D*, **74**, 123005, 2006 [astro-ph/0608017].
14. U. Seljak, A. Solsar and P. J. McDonald, *Cosmol. Astropart. Phys. JCAP*, **10**, 014, 2006 [astro-ph/0604335].
15. S. Dodelson, A. Melchiorri and A. Slosar, *Phys. Rev. Lett.*, **97**, 041301, 2006 [astro-ph/0511500].
16. K. N. Abazajian and G. M. Fuller, *Phys. Rev. D*, **66**, 023526, 2002 [astro-ph/0204293].
17. S. Dodelson, L. M. Widrow, *Phys. Rev. Lett.*, **72**, 17, 1994 [hep-ph/9303287].
18. A. D. Dolgov and S. H. Hansen, *Astropart. Phys.*, **16**, 339, 2002 [hep-ph/0009083].
19. K. Abazajian, G. M. Fuller, M. Patel, *Phys. Rev. D*, **64**, 023501, 2001 [astro-ph/0101524].
20. T. Asaka, M. Sahaposhnikov and A. Kusenko, *Phys. Lett. B*, **638**, 401, 2006 [hep-ph/0602150].
21. S. Sarkar, *Rept. Prog. Phys.*, **59**, 1493, 1996 [hep-ph/9602260].
22. K. Freese, E. W. Kolb, M. S. Turner, *Phys. Rev. D*, **27**, 1689, 1983.
23. R. Ruffini, D. J. Song, L. Stella, *Astron. Astrophys.*, **125**, 265, 1983.
24. R. Ruffini, D. J. Song, S. Taraglio, *Astron. Astrophys.*, **190**, 1, 1988.
25. C. J. Smith, G. M. Fuller, C. T. Kishimoto, K. N. Abazajian, *Phys. Rev. D*, **74**, 085008, 2006 [astro-ph/0608377].
26. Y. Z. Chu, M. Cirelli, *Phys. Rev. D*, **74**, 085015, 2006.
27. V. Kuzmin, V. Rubakov, M. Shaposhnikov, *Phys. Lett. B*, **155**, 36, 1985.
28. D. Falcone, F. Tramontano, *Phys. Rev. D*, **64**, 077302 2001 [hep-ph/0102136].
29. W. Buchmuller, P. Di Bari, M. Plumacher, 2004 *New Jour. Phys.*, **6**, 105 [hep-ph/0406014].
30. A. D. Dolgov, S. H. Hansen, S. Pastor, S. T. Petcov, G. Raffelt, D. V. Semikoz, *Nucl. Phys. B*, **632**, 363, 2002 [hep-ph/0201287].
31. Y. Y. Y. Wong, *Phys. Rev. D*, **66**, 025015, 2002 [hep-ph/0203180].
32. K. N. Abazajian, J. F. Beacom, N. F. Bell, *Phys. Rev. D*, **66**, 013008, 2002 [astro-ph/0203442].
33. D. N. Spergel et al. (WMAP collaboration), *Astrophys. J. Suppl.*, **170**, 377, 2007 [astro-ph/0603449].
34. Hinshaw et al. (WMAP Collaboration), *Astrophys. J. Suppl.*, **170**, 288, 2007 [astro-ph/0603451].
35. L. Page et al. (WMAP Collaboration), *Astrophys. J. Suppl.*, **170**, 335, 2007 [astro-ph/0603450].
36. G. Mangano, A. Melchiorri, O. Mena, G. Miele, A. Slosar, *J. Cosmol. Astropart. Phys.*, **JCAP03**, 006, 2007 [astro-ph/0612150].
37. K. A. Olive, E. D. Skillman, *Astrophys. J.*, **617**, 29, 2004 [astro-ph/0405588].

38. Y. I. Izotov, T. X. Thuan, G. Stasinska, *Astrophys. J.*, **662**, 15, 2007 [astro-ph/0702072].
39. K. Ichikawa, M. Kawasaki, K. Nakayama, M. Senami, F. J. Takahashi, *Cosmol. Astropart. Phys.*, **JCAP05**, 008, 2007 [hep-ph/0703034].
40. P. D. Serpico, G. G. Raffelt, *Phys. Rev. D*, **71**, 127301, 2005 [astro-ph/0506162].
41. Y. I. Izotov, T. X. Thuan, *Astrophys. J.*, **602**, 200, 2004 [astro-ph/0310421].
42. M. Lattanzi, R. Ruffini, G. V. Vereshchagin, *Phys. Rev. D*, **72**, 063003, 2006 [astro-ph/0509079].
43. K. Ichiki, M. Yamaguchi, J. Yokoyama, *Phys. Rev. D*, **75**, 084017, 2007 [hep-ph/0611121].
44. S. Hannestad, G. G. Raffelt, *J. Cosmol. Astropart. Phys.*, **JCAP11**, 016, 2006 [astro-ph/0607101].
45. M. Cirelli, A. J. Strumia, *Cosmol. Astropart. Phys.*, **JCAP12**, 013, 2006 [astro-ph/0607086].
46. K. Ichikawa, M. Kawasaki, F. J. Takahashi, *Cosmol. Astropart. Phys.*, **JCAP05**, 007, 2007 [astro-ph/0611784].
47. J. Hamann, S. Hannestad, G. G. Raffelt, Y. Y. Y. Wong, 2007 [arXiv:0705.0440].
48. M. Tegmark et al., (SDSS Collaboration), *Astrophys. J.*, **606**, 702, 2004 [astro-ph/0310725].
49. M. Tegmark et al., (SDSS Collaboration), *Phys. Rev. D*, **69**, 103501, 2004 [astro-ph/0310723].
50. P. McDonald et al., *Astrophysical J.*, **635**, 761, 2005 [astro-ph/0407377].
51. A. D. Dolgov, S. H. Hansen, A. Y. Smirnov, *J. Cosmol. Astropart. Phys.*, **JCAP06**, 004, 2005 [astro-ph/0611784].
52. A. de Felice, G. Mangano, P. D. Serpico, TroddenM, *Phys. Rev. D*, **74**, 103005, 2006 [astro-ph/0510359].
53. The Planck Consortia, *The Scientific Programme of Planck*, ESA-SCI 1, 2005 [astro-ph/0604069].
54. L. Lesgourgues, S. Pastor, *Phys. Rev. D*, **60**, 103521, 1999 [hep-ph/9904411].
55. M. Orito, T. Kajino, G. J. Mathews, Y. Wang, *Phys. Rev. D*, **65**, 123504, 2002 [astro-ph/0203352].
56. W. Hu, *Phys. Rev. D*, **62**, 043007, 2000 [astro-ph/0002238].
57. A. Challinor, A. Lewis, *Phys. Rev. D*, **71**, 103010, 2005 [astro-ph/0502425].
58. A. Lewis, A. Challinor, A. Lasenby, *Astrophys. J.*, **538**, 473, 2000 [astro-ph/9911177].
59. C. P. Ma, E. Bertschinger, *Astrophys. J.*, **455**, 7, 1995 [astro-ph/9401007].
60. U. Seljak, M. Zaldarriaga, *Astrophys. J.*, **469**, 437, 1996 [astro-ph/9603033].
61. R. Trotta, S. H. Hansen, *Phys. Rev. D*, **69**, 023509, 2004 [astro-ph/0306588].
62. S. Seager, D. D. Sasselov, D. Scott, *Astrophys. J.*, **523**, L1-L5, 1999 [astro-ph/9909275].
63. K. Ichikawa, T. Takahashi, *Phys. Rev. D*, **73**, 063528, 2006 [astro-ph/0601099].
64. P. D. Serpico, S. Esposito, F. Iocco, G. Mangano, G. Miele, O. Pisanti, *J. Cosmol. Astropart. Phys.*, **JCAP12**, 010, 2004 [astro-ph/0408076].
65. A. Lewis and S. Bridle, *Phys. Rev. D*, **66**, 103511, 2002 [astro-ph/0205436].
66. C. B. Netterfield et al., *Astrophys. J.*, **571**, 604, 2002 [astro-ph/0104460].
67. C. J. MacTavish et al., *Astrophys. J.*, **647**, 799, 2006 [astro-ph/0507503].
68. C. I. Kuo et al., *Astrophys. J.*, **600**, 32, 2004 [astro-ph/0212289].
69. A. C. S. Readhead et al., *Astrophys. J.*, **609**, 498, 2004 [astro-ph/0402359].
70. M. Tegmark et al., (SDSS Collaboration), *Phys. Rev.*, **74**, 123507 2006 [astro-ph/0608632].
71. W. J. Percival et al., *Astrophys. J.*, **657**, 645, 2007 [astro-ph/0608636].
72. S. Cole et al., (2dFGRS Collaboration), *Mon. Not. R. Astron. Soc.*, **362**, 505, 2002 [astro-ph/0501174].
73. P. Astier et al., *Astron. Astrophys.*, **447**, 31, 2006 [astro-ph/0510447].
74. A. G. Riess et al., *Astrophys. J.*, **607**, 665, 2004 [astro-ph/0402512].
75. W. L. Freedman et al., *Astrophys. J.*, **553**, 47, 2001 [astro-ph/0012376].
76. J. Hamann, J. Lesgourgues, G. Mangano, 2007, [astro-ph/0712.2826].
77. K. Ichikawa, T. Sekiguchi, T. Takahashi, 2007, [astro-ph/0712.4327].
78. P. Crotty, J. Lesgourgues, S. Pastor, *Phys. Rev. D*, **69**, 123007, 2004 [astro-ph/0302337].
79. \*\*\* <http://camb.info>.
80. \*\*\* <http://cosmologist.info/cosmomc>.